ARTICLE

A New Borate-phosphate Compound $CsNa_2Lu_2(BO_3)(PO_4)_2$: Crystal Structure and Tb^{3+} Doped Luminescence①

SHI Jian-Chao[a] WANG Hao[b②]
ZHANG Rui-Juan[a] ZHAO Dan[a②]
[a] (*College of Chemistry and Chemical Engineering, Henan Polytechnic University, Jiaozuo, Henan* 454000, *China*)
[b] (*School of Physics and Electronic Information Engineering, Henan Polytechnic University, Jiaozuo* 454000, *China*)

ABSTRACT Composite borate-phosphate compounds have always attracted much attention for their structure diversity and interesting properties. In this work, a new borate-phosphate $CsNa_2Lu_2(BO_3)(PO_4)_2$ (CNLBP) was found for the first time and its structure was characterized by single-crystal X-ray diffraction method. It crystallizes in orthorhombic system, space group *Cmcm* with a = 6.8750(5), b = 14.6919(1), c = 10.5581(7) Å, V = 1066.44(1) Å^3, Z = 4, M_r = 777.58, D_c = 4.843 g/cm^3, F(000) = 1368, μ(Mo$K\alpha$) = 22.20 mm^{-1}, $R(F^2 > 2\sigma(F^2))$ = 0.0173 and $wR(F^2)$ = 0.0367. The structure of CNLBP features a chain framework of $[Lu_2(BO_3)(PO_4)_2]_\infty$ that delimits 1D tunnels filled by Na^+ and Cs^+ ions. Phosphors CNLBP:xTb (x = 0, 0.1, 0.2, 0.4, 0.6, 0.8, 1.0) were prepared, and it can emit bright green light under near-UV excitation due to the $^5D_4 \rightarrow {}^7F_j$ (j = 6, 5, 4, 3) transition of Tb^{3+}. Due to the large separation of Lu^{3+} ions in CNLBP structure lattice, the optimal concentration of Tb^{3+} is 80%, and concentration quenching occurs only for the full Tb^{3+} concentration.

Keywords: borate-phosphate, crystal structure, photoluminescence, Tb^{3+};
DOI: 10.14102/j.cnki.0254-5861.2011-3284

1 INTRODUCTION

Inorganic borate and phosphate compounds possess a lot of interesting characteristics including low price, steady chemical property, various chemical structures and optically transparent in visible region[1-3]. The basic building block of phosphate compounds is PO_4 tetrahedron which is flexible and can inhibit various coordination environments by altering the P–O bond distances. The crystal structure of borate consists of BO_4 and BO_3 units, which can be linked together via common O atoms to give many structural species. It is conceivable that mixed borate-phosphate and polymerized borophosphate compounds possess more complicated and multitudinous structure types associated with interesting properties. So far, a large number of borate-phosphates and borophosphates have been reported, extending from isolated species, oligomers, rings, and chains to layers and frame-works[4-6]. These compounds known to date are systemically classified in terms of reviews by Kniep et al[7].

Rare-earth ions can be excited resonantly through $f \rightarrow f$ or $f \rightarrow d$ transitions or non-directly in charge transfer process or dipole-dipole energy transfer. If doping rare-earth ions into suitable host materials, promising phosphors would be given, which have become a hot topic in the recent twenty years[8-13]. As a typical representative, terbium is an old acquaintance to researchers for producing green-emitting phosphors. As is known to all, Tb^{3+} ion serves as an efficient green-emitting activator in a huge number of photoluminescence materials due to bright emission colors and high luminescent efficiencies when excited by charge transfer transitions in ultraviolet region[14, 15]. In this work, we started a searching for new borate-phosphate compound using high-temperature solution growth (HTSG) method, which is usually an effective method to prepare 0.2×millimeter-level crystals for structure

Received 10 June 2021; accepted 14 August 2021 (**CCDC 1950697**)
① This work was supported by the National Natural Science Foundation of China (No. 21201056)
② Corresponding authors. Wang Hao, born in 1985, Ph. D, associate professor, Tel: +86-13673919472, E-mail: wanghao@hpu.edu.cn
Zhao Dan, born in 1982, Ph.D, associate professor, Tel: +86-13839155305, E-mail: iamzd1996@163.com

determination by single-crystal X-ray diffraction (SC-XRD) method. We selected the mixture of Cs_2O–Na_2O–B_2O_3–P_2O_5 as flux and Lu_2O_3 as solvent. Surprisingly, a new borophosphate $CsNa_2Lu_2(BO_3)(PO_4)_2$ was successfully obtained. Meanwhile, we prepared Tb^{3+} doped phosphors $CsNa_2Lu_{2(1-x)}Tb_{2x}(BO_3)(PO_4)_2$ and studied the photoluminescence (PL) properties.

2 EXPERIMENTAL

2. 1 Materials and instrumentation

The synthesized materials Na_2CO_3 (AR ⩾ 99.0%), Cs_2CO_3 (AR ⩾ 99.0%), Lu_2O_3 (AR ⩾ 99.9%), Tb_4O_7 (AR ⩾ 99.9%), H_3BO_3 (AR ⩾ 99.0%) and $NH_4H_2PO_4$ (AR ⩾ 99.0%) were purchased from Aladdin Reagent Ltd. Co. (China). Phase structure analysis was performed with X-ray diffraction (XRD) equipment SmartLab 9KW diffractometer (Rigaku Co.) at room temperature. The 2θ range, scanning speed and step width for XRD measurement were set at 5~75°, 5 °/min, and 0.02 °/step. Solid-state ultraviolet-visible absorption spectra (UV-Vis) were measured using a spectrophotometer Hitachi UH4150 in the range of 240~780 nm. Photoluminescence performance was measured using an Edinburgh FLS1000 Fluorescence Spectrometer. The excitation source for steady-state emission and exciting spectra is a 500 W xenon lamp. The transient state fluorescence was measured using an EPL 365 nm laser. The electroluminescent (EL) properties of the prepared LED lamp were also measured with a FLS1000 testing system.

2. 2 Preparation

The high-temperature molten salt method, that is, flux method, was used to prepare small single crystals of compound CNLBP. Additional reactants Na_2CO_3, Cs_2CO_3, H_3BO_3 and $NH_4H_2PO_4$ in proper molar ratios were used as the flux to make sure melting of refractory Lu_2O_3. The raw materials, Cs_2CO_3 (1.303 g, 4 mmol), Na_2CO_3 (1.060 g, 10 mmol), Lu_2O_3 (0.0796 g, 0.2 mmol), H_3BO_3 (0.4177 g, 10 mmol) and $NH_4H_2PO_4$ (1.150 g, 10 mmol) were mixed and put into an arc platinum crucible after carefully grinding in an agate mortar. It was pre-treated in muffle furnace at 500 °C for 6 hours to release volatile gas (CO_2, NH_3, and H_2O). A necessary regrinding was performed to ensure the homogeneity of mixture. After that, the temperature was slowly increased to 850 °C to melt the mixture completely. After holding the temperature at 850 °C for 15 hours, the solution was cooled to 550 °C at a rate of 2 °C·h^{-1} to grow small single crystals. Finally, the production was washed by hot water to get rid of the addition flux. A few small single crystals of compound CNLBP can be carefully selected using a light microscope.

After proper structural analysis, pure powder samples of compounds $CsNa_2Lu_{2(1-x)}Tb_x(BO_3)(PO_4)_2$ (CNLBP:xTb; x = 0, 0.1, 0.2, 0.4, 0.6, 0.8, 1.0) were obtained quantitatively from the solid state reaction of Na_2CO_3, Cs_2CO_3, Lu_2O_3, Tb_4O_7, H_3BO_3 and $NH_4H_2PO_4$ in the stoichiometry ratio. The mixture was ground thoroughly in an agate mortar and pressed into a pellet. It was then calcined in a platinum crucible for 48 h at 760 °C, with several intermediate grinding stages ensuring a complete solid state reaction. Through XRD powder diffraction studies, it was proven that all seven samples were obtained successfully in a single phase (Fig. 1). The samples used for spectral measurements were polycry-stalline powders synthesized by solid-state reactions.

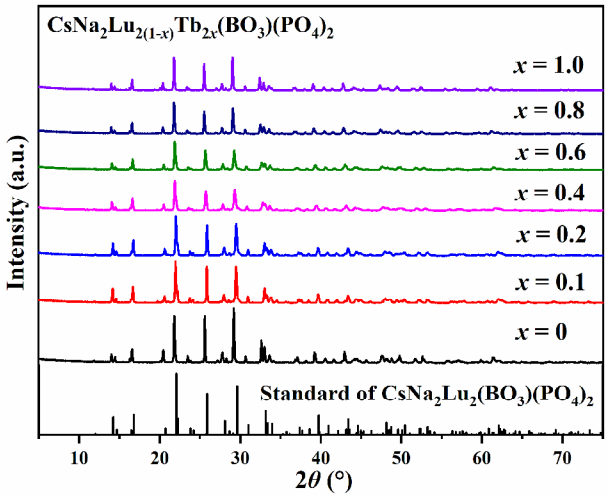

Fig. 1. XRD patterns of $CsNa_2Lu_{2(1-x)}Eu_{2x}(BO_3)(PO_4)_2$ (x = 0, 0.1, 0.2, 0.4, 0.6, 0.8, 1.0) samples

2. 3 Single-crystal X-ray diffraction

Single-crystal X-ray diffraction (SC-XRD) analysis was performed using the Bruker Smart Apex2 CCD device under the homeothermic condition of 20 ℃. The data were collected in the range from 3.27° to 28.25°, the exposure time was set as 10 second per deg and the scan width was set as 0.5°. Using this strategy, 1466 frames were collected in all for about six hours, and then the data were integrated with the Bruker Apex2 software package[16] using a narrow-frame integration algorithm. The unit cells were determined and refined by least-squares upon the refinement of XYZ-centroids of reflections above 3 times of $\sigma(I)$. Then the data were scaled for absorption using the SADABS programme of Apex2 package. Intensities of all measured reflections were corrected for *Lp* and multi-scan crystal absorption effects. The crystal structure of the title complex was solved by the Shelx-2017 crystallographic computing system[17]. All atoms were refined with anisotropic thermal parameters. The atomic coordinates and thermal parameters are given as Supporting information (Table S1, S2), and some important bond distances are summarized in Table S3.

3 RESULTS AND DISCUSSION

3. 1 Crystal structure description

As shown in Fig. 2a, CNLBP can be described as a three-chain framework of $[Lu_2(BO_3)(PO_4)_2]_\infty$ that delimits the 1D tunnels filled by Na^+ and Cs^+ ions. There is one unique caesium (I) atom, one unique sodium (I) atom, one unique lutecium (III) atom, one unique boron (III) atom, and one unique phosphorus (V) atom in each asymmetry unit. The B and P atoms form BO_3 and PO_4 coordination, respectively, and both BO_3 and PO_4 groups are isolated with each other. The B–O and P–O band distances are given in Table S3 (see supporting information), which are the common values within borate and phosphate compounds[18, 19]. The Lu atoms coordinate BO_3 and PO_4 to form a 3D open framework of $[Lu_2(BO_3)(PO_4)_2]_\infty$. All Lu atoms in this structure are surrounded by seven O atoms to form LuO_7 pentagonal bipyramids. Then each LuO_7 group connects with two adjacent LuO_7 via corner- and edge-sharing O atoms to form an infinite zig-zig $[Lu_2O_{13}]_\infty$ chain running along the *c*-axis, as shown in Fig. 2b. What is noticeable is that the B atom locates in the BO_3 plane with zero eccentricity ratio, and the Lu atoms exactly locate in the plane of LuO_7 pentagonal bipyramid. The Lu−O bond lengths fall in the range of 2.205(3)~2.449(4) Å. In this chain, each PO_4 group connects three LuO_7 groups.

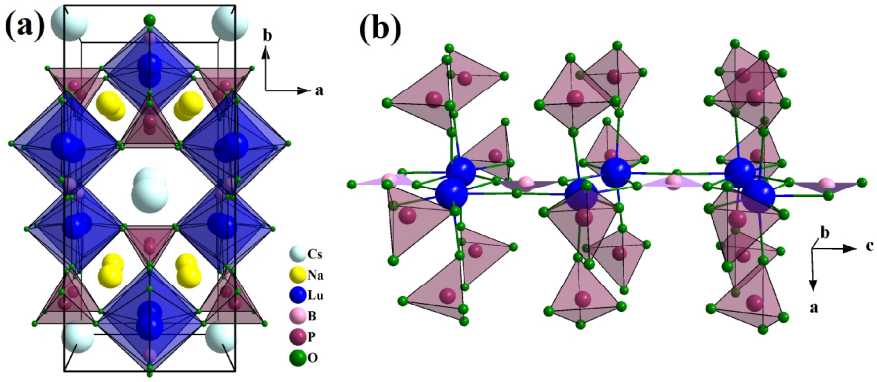

Fig. 2. (a) View of the crystal structure of $CsNa_2Lu_2(BO_3)(PO_4)_2$; (b) Chain framework of $[Y(BO_3)(PO_4)_2]_\infty$

Furthermore, large Cs and Na atoms locate among $[Lu_2(BO_3)(PO_4)_2]_\infty$ chains, connecting them and keeping up charge balance. Cs is surrounded by ten O atoms with the Cs–O distances of 3.236(3)~3.6556(1) Å, and the Na connects with seven O atoms with the Na–O distances of 2.286(3)~2.804(4) Å. These values are common within Na and Cs oxysalts[20]. Results of bond-valence calculations indicate that Cs, Na, Lu, B and P atoms are in reasonable oxidation states of +1, +1, +3, +3 and +5[21]. The calculated total bond valences are 0.842, 1.143, 3.018, 2.949 and 5.195 for Cs, Na, Lu, B and P atoms, respectively. This conclusion also supports the reasonability of our structure model for CNLBP.

3. 2 Luminescent properties

Fig. S1 (see supporting information) shows the UV-Vis absorbance spectrum of $CsNa_2Lu_2(BO_3)(PO_4)_2$. There is no absorbance above 400 nm, suggesting that the host material is optically transparent in the visible region. And thus, $CsNa_2Lu_2(BO_3)(PO_4)_2$ is suitable to be used as host lattice for rare-earth ion doping.

Fig. 3a shows the photoluminescence excitation (PLE) spectrum of $CsNa_2Lu_{1.2}Tb_{0.8}(BO_3)(PO_4)_2$. The PLE spectrum, which is recorded by monitoring with green emission peak at 541 nm, processes a series of spectral bands in the range of 200~450 nm. The broad excitation band at 250~290 nm is due to the band-to-band electronic transitions of CNLBP host material with further excitation transfer to Tb^{3+} dopant. The sharp peaks could be appropriately attributed to Tb^{3+}:4*f* → 4*f* forbidden transitions, i.e. $^7F_6$→ $^5H_6$ (304 nm), $^7F_6$ → $^5H_7$ (319 nm), $^7F_6$ → $^5D_2$ (354 and 360 nm), $^7F_6$ → $^5G_6$ (370 and 378 nm), and $^7F_6$ → $^5D_4$ at 487 nm[22]. Among these excitation peaks, the $^7F_6$ → $^5G_6$ transition at 378 nm shows the highest intensity. The photoluminescence emission (PL) spectrum of $CsNa_2Lu_{1.2}Tb_{0.8}(BO_3)(PO_4)_2$, which is excited by 378 nm light, is shown in Fig. 3b. Herein, the peaks arising in the green region at 487, 550, 582 and 628 nm are attributed to $^5D_4$ → ^7F_j (j = 6, 5, 4, 3) transition[23, 24] in turn. Among them, the $^5D_4$ → $^7F_5$ transition at 544 nm is the highest intensity, which suggests that the $CsNa_2Lu_{1.2}Tb_{0.8}(BO_3)(PO_4)_2$ can emit blue light under near-UV light excitation.

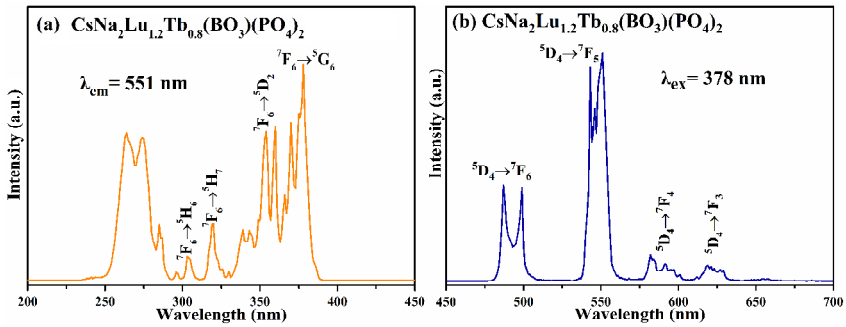

Fig. 3. PLE (a) and PL (b) spectra of $CsNa_2Lu_{1.2}Tb_{0.8}(BO_3)(PO_4)_2$ phosphor

To achieve the best concentration of Tb_{3+} activator, a series of powder samples $CsNa_2Lu_{2(1-x)}Tb_x(BO_3)(PO_4)_2$ (CNLBP:*x*Tb; *x* = 0, 0.1, 0.2, 0.4, 0.6, 0.8, 1.0) were prepared. As shown in Fig. 4, there was no obvious peak shift but the intensity changes with the variation of Tb^{3+} concentration. With increasing the concentration, the emission intensity increases and then reaches to the maximum at optimum concentration *x* = 0.8. For most phosphors, the luminous efficiency of Tb^{3+}-doped luminescent materials suffers greatly from the negative concentration quenching effect, leading to a low optimized concentration of Tb^{3+} (< 20%). However, this is negligibility in CNLBP:*x*Tb phosphor. The optimal concentration of Tb^{3+} is 80%, and the concentration quenching occurs only for the full Tb^{3+} concentration due to the large separation of Lu^{3+} ions in CNLBP structure lattice. As mentioned above, the Lu^{3+} ions are in a linear array, and the nearest distance between neighbouring interline Lu^{3+} ions is 3.5492(2) Å, whereas the nearest intraline Lu^{3+}–Lu^{3+} distance is 5.9664(4) Å. Even doping large concentration of Tb^{3+} in Lu^{3+} sites, energy migration between Tb^{3+} ions will no longer occur freely for the large separation of intraline Tb^{3+} ions. This will greatly reduce the possibility of the effective energy to be captured by quenching centres, even for 80% Tb^{3+} concentration. Hence, we suppose that the CNLBP host can accommodate high concentration of Tb^{3+} ions with neglectable concentration quenching.

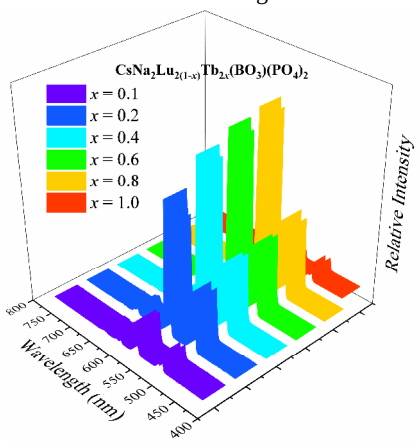

Fig. 4. PL spectra of CNLBP:*x*Tb (*x* = 0, 0.1, 0.2, 0.4, 0.6, 0.8, 1.0) phosphors by 378 nm excitation

In order to further prove the minor concentration quenching in phosphors CNLBP:*x*Tb, the room temperature decay curves of CNLBP:*x*Tb phosphors with respect to the $^5D_4 \rightarrow {}^7F_5$ emission of Tb^{3+} by 378 nm excitation was studied. All average decay curves can be well fitted with the mono-exponential Eq. (1)[25, 26]:

$$I_{(t)} = I_0 \exp(-t/\tau) \quad (1)$$

where t is the time, τ presents the decay time, $I_{(t)}$ and I_0 are the emission intensity at time t and 0. Typically, the specified fitting lifetime values of CNLBP:*x*Tb are 2.21, 2.12, 1.97, 1.82, 1.76 and 1.14 ms for x = 0.1, 0.2, 0.4, 0.6, 0.8 and 1.0 correspondingly (Fig. 5). It is evident that the decay time decreases very slowly with increasing x from 0.1 to 0.8, owing to the increase of non-radiative decay rate of internal Tb^{3+} and the absence of concentration quenching. When x is 1.0, larger than 0.8, the decay time drops quickly from 1.76 to 1.14 ms, suggesting the appearance of concentration quenching.

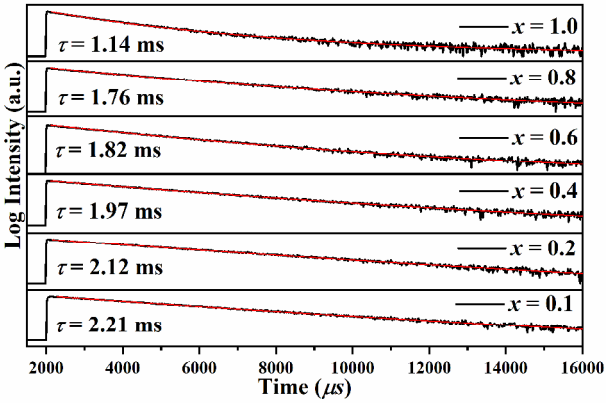

Fig. 5. Comparison of the fluorescent decay curves of CNLBP:*x*Tb (x = 0, 0.1, 0.2, 0.4, 0.6, 0.8, 1.0)

3. 3 Chromaticity coordinates

It is well-known that three main colors recognized by the human vision system are red, green and blue[27-29]. These three colors are usually referred to as the Commission Internationale de l´Eclairage (CIE) 1931 color coordinates, which is the current standard for lighting specifications on the market. In general, the color of any light source in this color space can be represented as an (x, y) coordinate. The location of the color coordinates of $CsNa_2Lu_{1.2}Tb_{0.8}(BO_3)(PO_4)_2$ phosphor on the CIE chromaticity diagram is presented in Fig. 6. Under excitation at 378 nm, the calculated CIE chromaticity coordinate is (0.3117, 0.6033), falling in the green region. Thus, we may expect that compound $CsNa_2Lu_{1.2}Tb_{0.8}(BO_3)(PO_4)_2$ can be used as a good green phosphor for white LED.

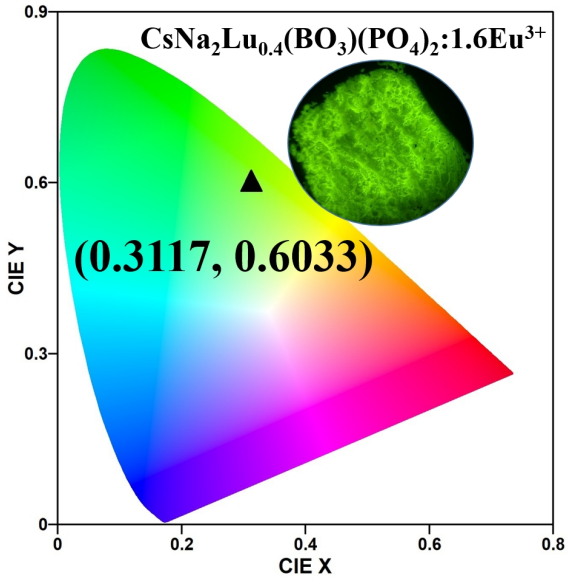

Fig. 6. Chromaticity coordinates of $CsNa_2Lu_{1.2}Tb_{0.8}(BO_3)(PO_4)_2$ phosphor in the CIE 1931 chromaticity diagram

4 CONCLUSION

For the first time, a new borate phosphate $CsNa_2Lu_2(BO_3)(PO_4)_2$ was discovered by high temperature flux method, and its crystal structure was determined by SC-XRD method. The structure can be described as a chain framework of $[Lu_2(BO_3)(PO_4)_2]_\infty$ that delimits 1D tunnels filled by Na^+ and Cs^+ ions. Then Tb^{3+} ion was introduced to prepare a series of phosphors CNLBP:*x*Tb (*x* = 0, 0.1, 0.2, 0.4, 0.6, 0.8, 1.0), and it can emit bright green light under near-UV excitation due to the $^5D_4 \rightarrow {}^7F_j$ (j = 6, 5, 4, 3) transition of Tb^{3+}. Owing to the large separation of Lu^{3+} ions in CNLBP structure lattice, the optimal concentration of Tb^{3+} is 80%, and concentration quenching occurs only for the full Tb^{3+} concentration. Therefore, we can say that CNLBP host can accommodate high concentration of Tb^{3+} ions with neglect-table concentration quenching.

REFERENCES

(1) Mutailipu, M.; Poeppelmeier, K. R.; Pan, S. Borates: a rich source for optical materials. *Chem. Rev.* **2021**, 121, 1130–1202.

(2) Zhang, W. L.; Guo, Z. G.; Zhang, H.; Hancock, J.; Ding, F. H.; Chen, X.; Li, X. Y.; Cheng, W. D. Incorporation of three kinds of borate anionic groups in one single copper oxyborate including the unprecedented branched anionic $(B_3O_7)^{5-}$ group. *Mater. Res. Bull.* **2019**, 117, 84–89.

(3) Zhao, D.; Zhang, S. R.; Fan, Y. P.; Liu, B. Z.; Li, Y. N.; Shi, L. Y.; Dai, S. J. Two-site occupancy induced a broad-band emission in phosphor $K_2YZr(PO_4)_3:Eu^{2+}$ for white-light-emitting diode applications. *ACS Sustain. Chem. Eng*. **2020**, 8, 18992–19002.

(4) Shvanskaya, L. V.; Yakubovich, O. V.; Belik, V. I. New type of borophosphate anionic radical in the crystal structure of $CsAl_2BP_6O_{20}$. *Crystallog. Rep.* **2016**, 61, 786–795.

(5) Hasegawa, T.; Yamane, H. Synthesis and crystal structure analysis of $Li_2NaBP_2O_8$ and $LiNa_2B_5P_2O_{14}$. *J. Solid State Chem.* **2015**, 225, 65–71.

(6) Wang, Y.; Pan, S.; Huang, S.; Dong, L.; Zhang, M.; Han, S.; Wang, X. Structural insights for the design of new borate-phosphates: synthesis, crystal structure and optical properties of $Pb_4O(BO_3)(PO_4)$ and $Bi_4O_3(BO_3)(PO_4)$. *Dalton Trans.* **2014**, 43, 12886–12893.

(7) Kniep, R.; Engelhardt, H.; Hauf, C. A first approach to borophosphate structural chemistry. *Chem. Mater.* **1998**, 10, 2930–2934.

(8) Zhao, D.; Xue, Y. L.; Zhang, S. R.; Shi, L. Y.; Liu, B. Z.; Fan, Y. P.; Yao, Q. X.; Dai, S. J. Non-concentration quenching, good thermal stability and high quantum efficiency of $K_5Y(P_2O_7)_2:Eu^{3+}/Tb^{3+}$ phosphors with a novel two-dimensional layer structure. *J. Mater. Chem. C* **2019**, 7, 14264–14274.

(9) Ji, Q. S.; Wen, W. F.; Liu, S. Z.; Liu, X.; He, L. F.; Yi, X. G.; Chen, W. T. Series of novel lanthanide complexes with a ladder-shaped 1-D double chain: preparation, structures and photophysical properties. *Inorg. Chim. Acta* **2021**, 519, 120278-1-7.

(10) Xu, X.; Liu, X.; Wang, D.; Liu, X.; Chen, L.; Zhao, J. $\{HPO_3\}$ and $\{WO_4\}$ simultaneously induce the assembly of tri-Ln(III)-incorporated antimonotungstates and their photoluminescence behaviors. *Inorg. Chem.* **2021**, 60, 1037–1044.

(11) Liu, J.; Wang, D.; Xu, X.; Li, H.; Zhao, J.; Chen, L. Multi-nuclear rare-earth-implanted tartaric acid-functionalized selenotungstates and their fluorescent and magnetic properties. *Inorg. Chem.* **2021**, 60, 2533–2541.

(12) Xu, X.; Li, H.; Xie, S.; Mei, L.; Meng, R.; Chen, L.; Zhao, J. Double-oxalate-bridging tetralanthanide containing divacant lindqvist isopolytungstates with an energy transfer mechanism and luminous color adjustablility through Eu^{3+}/Tb^{3+} codoping. *Inorg. Chem.* **2020**, 59, 648–660.

(13) Xu, X.; Meng, R.; Lu, C.; Mei, L.; Chen, L.; Zhao, J. Acetate-decorated tri-Ln(III)-containing antimonotungstates with a tetrahedral $\{WO_4\}$ group as a structure-directing template and their luminescence properties. *Inorg. Chem.* **2020**, 59, 3954–3963.

(14) Wen, G. X.; Han, M. L.; Wu, X. Q.; Wu, Y. P.; Dong, W. W.; Zhao, J.; Li, D. S.; Ma, L. F. A multi-responsive luminescent sensor based on a super-stable sandwich-type terbium(III)-organic framework. *Dalton Trans.* **2016**, 45, 15492–15499.

(15) Xu, X.; Lu, C.; Xie, S.; Chen, L.; Zhao, J. A trimeric tri-Tb^{3+} including antimonotungstate and its $Eu^{3+}/Tb^{3+}/Dy^{3+}/Gd^{3+}$-codoped species with luminescence properties. *Dalton Trans.* **2020**, 49, 12401–12410.

(16) Bruker, APEX2 and SAINT, Bruker AXS Inc., Madison, Wisconsin, USA **2017**.

(17) Sheldrick, G. M. A short history of SHELX, *Acta Crystallogr. Sec. C* **2015**, 71, 3–8.

(18) Li, X. B.; Hu, C. L.; Kong, F.; Mao, J. G. $Ba_3Sb_2(PO_4)_4$ and $Cd_3Sb_2(PO_4)_4(H_2O)_2$: two new antimonous phosphates with distinct $Sb(PO_4)_2$ structure types and enhanced birefringence. *Inorg. Chem.* **2021**, 60, 1957–1964.

(19) Feng, J.; Xu, X.; Hu, C. L.; Mao, J. G. $K_6ACaSc_2(B_5O_{10})_3$ (A = Li, Na, $Li_{0.7}Na_{0.3}$): nonlinear-optical materials with short uv cutoff edges. *Inorg. Chem.* **2019**, 58, 2833–2839.

(20) Zhao, D.; Ma, F.; Zhang, R.; Zhang, R.; Zhang, L.; Fan, Y. Crystal structure and luminescence properties of self-activated phosphor $CsDyP_2O_7$. *Mater.*

Res. Bull. **2017**, 87, 202–207.

(21) Brese, N. E.; O'Keeffe, M. Bond-valence parameters for solids. *Acta Crystallogr. Sec. B* **1991**, 47, 192–197.

(22) Chen, W. T. Preparation, structure and properties of $[Tb(HIA)_2(IA)(H_2O)_2(HgCl_2)]_n(nHgCl_4)\cdot 3nH_2O$ (IA = isonicotinate anion). *J. Chem. Crystallogr.* **2021**, 51, 116–123.

(23) Xu, X.; Xie, S.; Yang, G.; Zhao, J. Tetrahedral $\{HPO_3\}$ and $\{WO_4\}$ group simultaneously directing tri-Tb(III)-containing antimonotungstate and its photoluminescence properties. *Inorg. Chem. Commun.* **2020**, 119, 108073-1-6.

(24) Xue, Y. L.; Zhao, D.; Shi, C. L.; Liu, B. Z.; Zhao, J.; Li, F. F. Energy transfer and green emitting properties of solid solution $PbGd_{1-x}Tb_xB_7O_{13}$ (x = 0 similar to 1). *Chin. J. Struct. Chem.* **2018**, 37, 1279–1286.

(25) Zhao, Y.; Wang, Y. J.; Wang, N.; Zheng, P.; Fu, H. R.; Han, M. L.; Ma, L. F.; Wang, L. Y. Tetraphenylethylene-decorated metal-organic frameworks as energy-transfer platform for the detection of nitro-antibiotics and white-light emission. *Inorg. Chem.* **2019**, 58, 12700–12706.

(26) Dang, P.; Li, G.; Yun, X.; Zhang, Q.; Liu, D.; Lian, H.; Shang, M.; Lin, J. Thermally stable and highly efficient red-emitting Eu^{3+}-doped $Cs_3GdGe_3O_9$ phosphors for WLEDs: non-concentration quenching and negative thermal expansion. *Light: Sci. Appl.* **2021**, 10, 29-1-13.

(27) Chen, W. T. Synthesis, structure, photoluminescence, band gap and energy transfer mechanism of a novel bimetallic thulium-mercury compound with a three-dimensional framework. *J. Iran. Chem. Soc.* **2021**, 18, 181–189.

(28) Liu, S. Z.; Chen, Y. Q.; Peng, H. Q.; Ji, Q.; Wang, X. X.; Wei, L.; Zhong, Q. Y.; Chen, W. T. *In situ* preparation and photophysical properties of a novel europium complex. *J. Solid State Chem.* **2021**, 299, 122170.

(29) Ji, Q. S.; Wen, W. F.; Liu, S. Z.; Liu, X.; He, L. F.; Yi, X. G.; Chen, W. T. Series of novel lanthanide complexes with a ladder-shaped 1-D double chain: preparation, structures and photophysical properties. *Inorg. Chim. Acta* **2021**, 519, 120278-1-7.